University of Modena and Reggio Emilia
Department of Engineering "Enzo Ferrari"

Master's Degree in Automotive Engineering
Automotive Fluid Power Systems

Modeling and Simulation of a MotoGP Holeshot Device Hydraulic System

Nicolas Romanella
Marcello Mazzoleni

Professor Barbara Zardin
Academic Year 2024/25



December 19th, 2024

Summary

This report presents the modeling and simulation of a hydraulic system using the lumped parameter approach, conducted for the course "Automotive Fluid Power Systems" as part of the Master's Degree in Automotive Engineering at the University of Modena and Reggio Emilia. The aim of this study is to design and simulate the complete hydraulic circuit of a MotoGP holeshot device. The analysis focuses on the ride height device first introduced by Ducati in 2022, specifically examining its functionality in holeshot mode during the start phase. Several dynamic effects have been intentionally disregarded in order to simplify the analysis and emphasize the hydraulic aspects, as required by the course objectives.

Contents

1 Introduction **5**

1.1 Holeshot device history 5

1.2 Project implementation 6

2 Dynamic analysis **7**

2.1 Data collection 7

2.2 Simulation parameters 7

2.3 Rear suspension model 9

2.4 Front suspension model 12

3 OpenModelica **14**

3.1 Working fluid 14

3.2 Generation group 14

3.3 Fluid volume estimation 16

3.4 Distribution group 18

3.5 Execution group 19

4 Main results **21**

4.1 Pressure and stroke behavior 21

4.2 Complete circuit layout 22

1 Introduction

1.1 Holeshot device history

The lowering devices used in MotoGP are mechanical systems that allow the adjustment of a motorcycle's height either during motion or at the start of a race, thereby enhancing performance. These systems, operated by the rider through a lever or a button, function by lowering either the rear (rear lowering device) or the front (front lowering device) of the motorcycle. This adjustment helps optimizing stability during acceleration and reduces the risk of wheelies. The devices automatically deactivate upon the first application of the brakes.

Ducati introduced the first rear lowering device on the GP19, initially designed to enhance race starts (referred to as "holeshot device"). This innovation marked a turning point, with subsequent developments enabling its use during flying laps to improve acceleration when exiting corners. Ducati later developed a front lowering device, expanding the concept to further optimize starting procedures. Subsequently, they unveiled an advanced front system, known as the "ride height device," which could be utilized during race laps. This groundbreaking innovation prompted other teams to develop similar systems to stay competitive.



Figure 1: Ducati GP19 holeshot device initiation lever.

Despite its technical success, the front lowering device was banned starting from the 2023 season, as decided by the GP Commission during the meeting held on March 18, 2022. The updated regulations prohibit any device that modifies the front height of the motorcycle while in motion, allowing such systems solely for starting procedures. The primary reasons behind the ban include alleged increases in rider risks, high development

costs, and the lack of practical applications for road vehicles. However, it was noted that other technologies present in MotoGP, such as carbon brakes or seamless gearboxes, also lack direct applicability for road use, highlighting a controversial interpretation of the regulations:

> *The use of any device that modifies or adjusts the front height of the motorcycle while in motion is prohibited. The decision of the Technical Director will be final in determining what constitutes a 'ride height device'. Such devices are permitted only at the start of a race (i.e. 'holeshot' devices).*

1.2 Project implementation

In this study, the objective is to design a ride height device system. However, to avoid excessively complicate the analysis and to maintain focus on developing the hydraulic circuit layout, we will simulate the device exclusively in its holeshot function, for lowering the motorcycle during starting procedures. This approach allows us to concentrate on the analysis and sizing of the hydraulic circuit required for the system's operation, ensuring a detailed and coherent treatment aligned with the project's educational objectives.

Given the nature of the project and the specific focus on the lowering function for the start, we will henceforth refer to the system as the 'holeshot device'. This terminology better reflects the scoped nature of our study and helps maintain consistency in the technical description of the project.

2 Dynamic analysis

2.1 Data collection

The secrecy surrounding these devices poses a significant barrier to their analysis. Most of the available information comes from indirect observations or limited technical statements, which is why we will rely on reasonable estimations and images circulating online. Some sources suggest that Ducati's front lowering device enables a reduction of the center of gravity by approximately 30–40 mm, significantly improving traction when exiting corners. For the rear, similar or slightly greater values could be achieved, given the easier implementation compared to the front.

In detailed images of race motorcycles, such as the Ducati Desmosedici GP24, it is evident that during starts the system lowers the motorcycle so much that the lower fairing nearly touches the ground. This effect is particularly noticeable when both the front and rear devices are activated simultaneously. Consequently, we estimate a total center-of-gravity lowering of approximately 50 mm, derived from the lowering of both front and rear by the same amount.

2.2 Simulation parameters

Defining the motorcycle geometries is a crucial step in this project, as they directly influence dynamic behavior, grip, stability, vehicle agility, and, most importantly, the distribution of weights and forces acting on the actuators. We will consider the following key parameters, based on typical values for a MotoGP motorcycle:

- The wheelbase has been set to approximately $l = 1450\,\text{mm}$, a standard value for competition motorcycles, which strikes a balance between stability at high speeds and maneuverability during direction changes.
- The center of mass height of the motorcycle and rider system has been estimated at $h = 550\,\text{mm}$ from the ground. This parameter is critical for dynamic stability: a lower center of mass enhances stability, while a higher one improves agility.
- The total mass of the motorcycle and rider system has been assumed to be $m = 230\,\text{kg}$, considering the minimum regulatory weight for a MotoGP motorcycle (157 kg) and an average of 65-80 kg for the rider in full gear.

The simulation will last 15 seconds. The dynamic effects of transients and the chain pull effect are neglected, with load transfers assumed to be ideal and represented by linear trends described through a piecewise linear function.

MotoGP motorcycles are capable of achieving longitudinal accelerations of up to 1.5-1.8 g due to optimized traction and electronic control. However, the simulated test will replicate a non-aggressive start, broken down into the following phases:

- Activation of the front and rear lowering devices via dedicated control;
- Acceleration up to the wheelie limit;
- Braking near the tipping limit;
- Deactivation of the front and rear lowering devices;
- Complete vehicle stop.

It is assumed that, under static conditions, the total weight of the system is:

$$F = 230\,\mathrm{kg} \cdot 9.81\,\mathrm{m/s^2} = 2256\,\mathrm{N}$$

distributed equally between the front and rear. In the figure, the 50-50 split is taken as the 100% condition for both the front and rear. During acceleration, a load transfer to the rear is assumed, resulting in 90% of the weight being transferred to the rear and 10% to the front. Conversely, during braking, the situation reverses, with 90% of the weight transferred to the front and 10% to the rear.

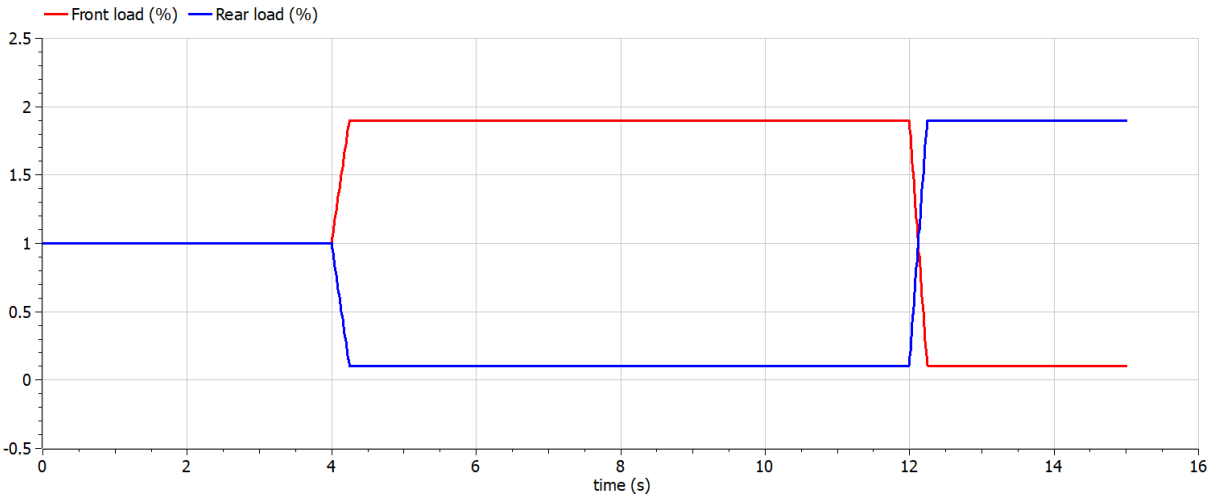


Figure 2: Load transfer during the complete maneuver.

To ensure greater realism, the linear functions describing the load transfers include a defined time duration for each phase, allowing for gradual rather than instantaneous variation. This choice improves the representation of physical phenomena while maintaining a simplified approach.

2.3 Rear suspension model

We chose to model the rear suspension using the ProLink-Honda kinematics, a progressive linkage system commonly used in sport and competition motorcycles. This configuration is valued for its ability to provide progressive behavior, meaning an increase in suspension stiffness as compression increases. This allows for optimal handling of both small surface irregularities and more violent impacts, thus enhancing comfort and traction. These types of suspensions are characterized by a linkage that amplifies the rear wheel travel relative to the shock absorber compression, thereby improving the motorcycle's control and sensitivity, although at the cost of higher reactive forces between the various components.

For our project, we derived the typical geometries of this suspension from available images online, adapting them to the model's requirements. The lowering of the motorcycle is achieved by adjusting the linkage, which in our case was extended by 20 mm with a linear hydraulic actuator to generate a vertical wheel travel of 51.8 mm. The progressive nature and leverage of this architecture allow for a greater wheel travel than that directly induced by the linkage.

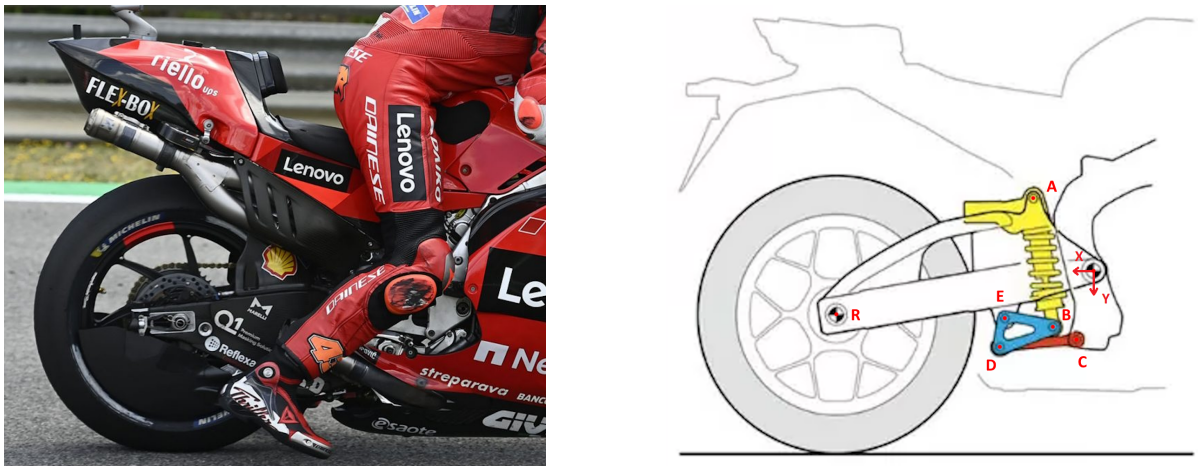


Figure 3: Rear suspension linkage design from picture.

The kinematics are constrained to the frame (assumed to be fixed) at points **A**, **O**, and **C**. The distribution of the weight force is defined by the upward reaction of the wheel on the pivot attached to the swingarm at point R. To accurately represent this mechanism, we developed a position analysis using a MATLAB code. The calculation is based on solving the articulated quadrilateral ABDC as a function of the shock absorber angle, followed by determining the coordinates of point **E**, which is common to both the rocker and the swingarm, through the intersection of circles defined by the vectors **OE** and **BE**.

All the necessary measurements were derived from the drawing in Figure 3, which is scaled relative to the 17-inch diameter of the rear wheel. The main dimensions used are as follows:

- **Point A (Frame):** Fixed at $[130, -158]$
- **Point C (Frame):** Fixed at $[38, 148]$
- **Point O (Frame):** Fixed at $[0, 0]$
- **Rod AB (Spring):** 281 mm
- **Rod BD (Rocker):** 123 mm
- **Rod BE (Rocker):** 105 mm
- **Rod DE (Rocker):** 64 mm
- **Rod OE (Swingarm):** 216 mm
- **Rod OR (Swingarm):** 562 mm
- **Rod ER (Swingarm):** 363 mm
- **Linkage Initial Length:** 165 mm

To determine the reaction forces at the key points of the frame, we used the equilibrium equations for both rotational and translational forces. These equations allow for the calculation of the forces acting at critical locations, specifically at the nodes of the frame. The goal was to find the reaction force at the linkage in point **C** and the reaction at the spring in point **A**.

Equilibrium of the swingarm rotation:

$$\mathbf{OR} \times \mathbf{F_R} + \mathbf{OE} \times \mathbf{F_E} = 0$$

Equilibrium of the rocker rotation:

$$\mathbf{EB} \times \mathbf{F_B} + \mathbf{ED} \times \mathbf{F_D} = 0$$

Equilibrium of the rocker translation:

$$\mathbf{F_D} + \mathbf{F_E} + \mathbf{F_B} = 0$$

In the hypothesis of a 2D problem with perfectly rigid bodies and the known directions **AB** and **CD** of the forces $\mathbf{F_B}$ and $\mathbf{F_D}$) in the working condition shown in the figure, the system is isostatic and solvable using the four equations for the four unknowns $\mathbf{F_B}$, $\mathbf{F_D}$, and $\mathbf{F_E}$. The calculation will be performed for two stages of the suspension in the static working condition: the first with the linkage at its initial length of 165 mm, and the second with the linkage extended by 20 mm.

Initial Linkage (165 mm):

$$\mathbf{F_E} = [3264, -1543]\,\text{N}, \quad \mathbf{F_B} = [-281, 1836]\,\text{N}, \quad \mathbf{F_D} = [-2983, -294]\,\text{N}$$

Tensile force on linkage: 2998 N, Compression force on spring: 1858 N

Extended Linkage (185 mm):

$$\mathbf{F_E} = [3027, -1909]\,\text{N}, \quad \mathbf{F_B} = [-185, 1825]\,\text{N}, \quad \mathbf{F_D} = [-2843, 84]\,\text{N}$$

Tensile force on linkage: 2844 N, Compression force on spring: 1835 N

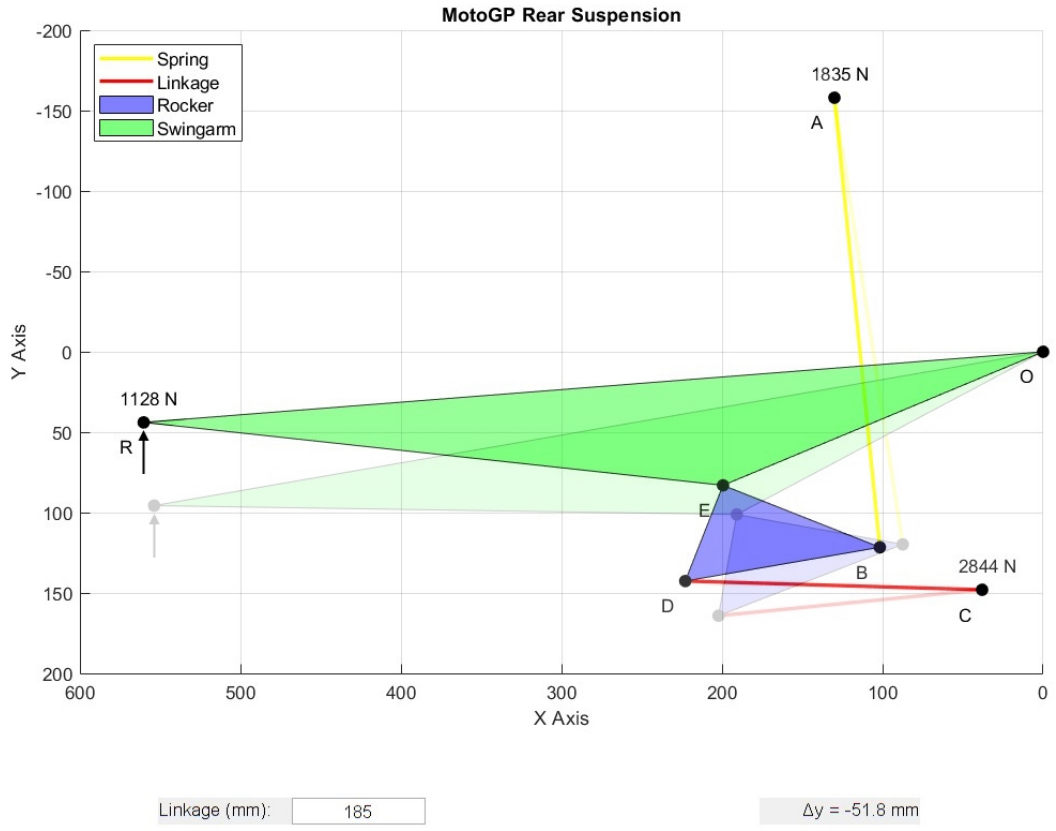


Figure 4: Rear suspension kinematics in static working conditions.

Considering the shock absorber already in working condition, and thus compressed, the forces acting on it during the stroke vary in a limited way. Oscillations on the order of 23 N on an elastic element with a stiffness of about 70 N/mm generate negligible geometric variations. Regarding the overall equilibrium of the structure, the linkage is in tension with a force of 2998 N in the standard static condition and 2844 N with the lowering device engaged. For the simulation, we will conservatively adopt the higher value between the two to ensure greater safety and reliability in the analysis.

2.4 Front suspension model

While the rear lowering device can be easily modeled by replacing the linkage with a linear hydraulic actuator, the front lowering device presents greater complexity. This system, in fact, operates by adjusting the preload of the suspension, effectively transforming it into an active suspension. Consequently, there are various technological solutions, some more economical and others more sophisticated, which are adopted confidentially by each manufacturer to maintain a competitive edge. This variety of approaches is due to the need to balance effectiveness, weight, reliability, and costs, in addition to considerations related to technical regulations and industrial secrecy. If other reasons or technical motivations exist, they may include the difficulty of integrating the system without compromising the structural rigidity or the dynamic response of the motorcycle.

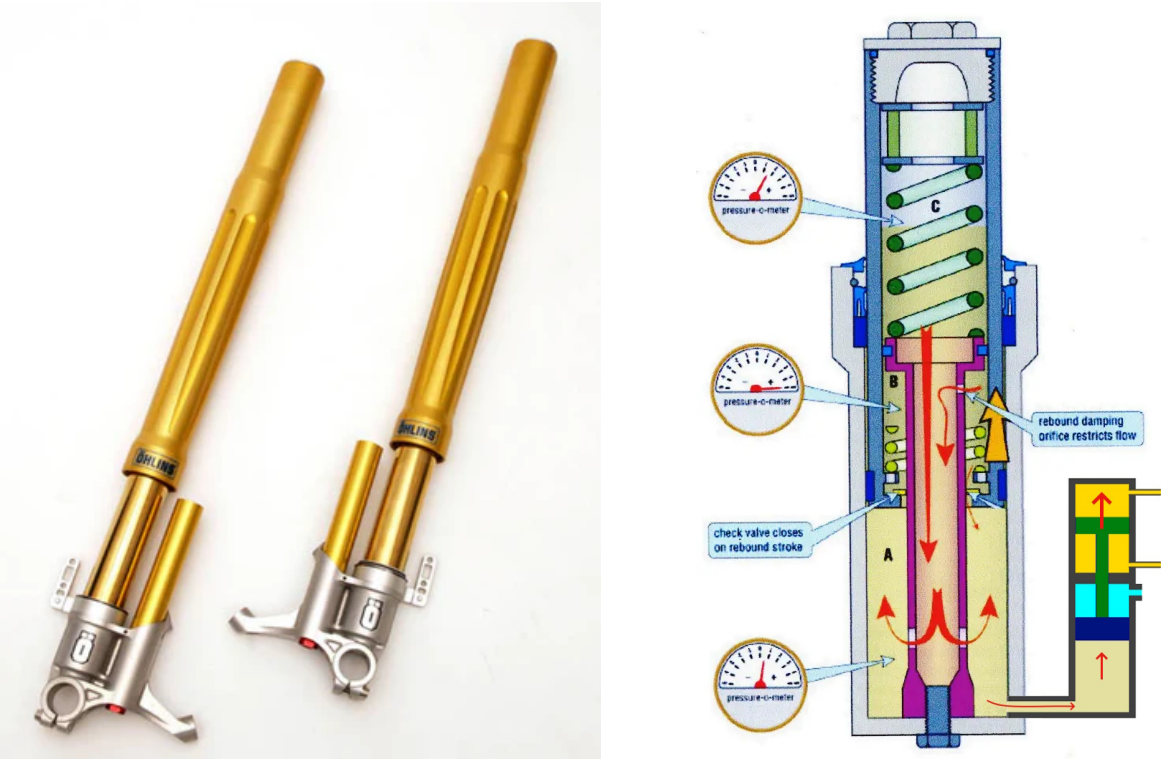


Figure 5: Front suspension hypothetical design.

In light of this, we propose a very simple solution, which involves expanding the oil chamber integrated with the fork's foot through the implementation of a linear actuator connected to the hydraulic circuit. This actuator will move a piston that separates the oil chamber, coming from the fork shaft, from the air chamber at atmospheric pressure. The latter will serve only as the travel space for the piston, so it is sufficient to ensure it remains free of contamination. The third chamber, in which the actuator moves, must be perfectly sealed from the oil chamber to prevent contamination of the hydraulic circuit with air. When the lower chamber of the actuator is pressurized, the piston moves vertically, increasing the fluid volume. This generates a low pressure that draws oil from the fork, compressing it together with the spring, which will provide elastic resistance.

In static conditions, the compression of the spring would cause a reduction in the available volume within the fork tube, as the shaft occupies part of the space, pushing the oil towards the secondary chamber and keeping the piston under pressure. Since, in the absence of loads on the suspension, the oil would not be under pressure, the static pressure load acting on the piston can be modeled as equivalent to the preloaded spring load, including the contribution of the damper to account for dynamic effects.

To ensure the conservation of volume under the assumption of incompressible oil fluid, the displacement of the piston in the actuator cylinder is proportional to the displacement of the shaft, based on the area ratio:

$$A_{\text{piston}} \cdot x_{\text{piston}} = A_{\text{shaft}} \cdot x_{\text{shaft}}$$

For simplicity of calculation, we assume $A_{\text{piston}} = A_{\text{shaft}}$. Consequently, the piston displacement will be equal to the shaft displacement. With $x_{\text{piston}} = 60\,\text{mm}$, we obtain $x_{\text{shaft}} = 60\,\text{mm}$. Taking into account a rake angle $\theta = 23°$, the vertical lowering of the motorcycle is:

$$h = x_{\text{shaft}} \cdot \cos(\theta) = 55.2\,\text{mm}.$$

The spring stiffness has been set to 10 N/mm, a common value that ensures a good compromise between support and flexibility. The spring preload has been set to 8 mm, ensuring the correct working position of the fork under standard riding conditions. The overall damping has been chosen as 1800 N/mm/s, representing an average of typical values for two forks in parallel. The static load acting in the longitudinal direction of the shaft is:

$$F = 1128\,\text{N} \cdot \cos(\theta) = 1038\,\text{N}$$

3 OpenModelica

3.1 Working fluid

The oil used in MotoGP lowering devices is generally a high-performance racing hydraulic oil, often produced by specialized brands such as Öhlins, Motul, Liqui Moly, or Maxima. One of the most commonly used oils for these purposes is the Öhlins R&T 1309, specifically designed for high-stress applications, such as advanced suspension and hydraulic systems.

It has the following characteristics:

- Low viscosity: Often classified as SAE 2.5W or lower, to ensure maximum reactivity and smoothness. The kinematic viscosity is typically below 15 cSt at 40°C.
- High thermal stability: Maintains performance over a wide temperature range, from very low temperatures (to prevent gelling) to very high temperatures (to resist overheating).
- Low compressibility: Essential for lowering systems, where precision in force and motion transfer is required.
- Advanced additive formulation: Contains anti-wear, anti-foam, and antioxidant additives for longer durability and consistent performance.

3.2 Generation group

To determine the required working pressure, the values were calculated based on the static load required by the suspension and the dimensions of the actuators. For the rear lowering device, with a 40 mm piston, a 10 mm shaft, and a load of 2998 N, the calculated pressure is 25.45 bar; for the front lowering device, with a 25 mm piston, a 10 mm shaft, and a load of 1038 N, the pressure is 25.17 bar. Both calculations are based on the effective area of the piston and confirm that a standard working pressure of 26 bar is adequate to ensure the proper functioning of the hydraulic systems.

$$A_{\text{net, rear}} = \pi \cdot \left(\frac{40}{2}\right)^2 - \pi \cdot \left(\frac{10}{2}\right)^2 = 1178\,\text{mm}^2 \quad \rightarrow \quad p_{\text{rear}} = \frac{2998\,\text{N}}{1178\,\text{mm}^2} = 25.45\,\text{bar}$$

$$A_{\text{net, front}} = \pi \cdot \left(\frac{25}{2}\right)^2 - \pi \cdot \left(\frac{10}{2}\right)^2 = 412\,\text{mm}^2 \quad \rightarrow \quad p_{\text{front}} = \frac{1038\,\text{N}}{412\,\text{mm}^2} = 25.17\,\text{bar}$$

The volumes of fluid required to move the actuators in 0.5 seconds are:

Actuator	Piston	Shaft	Stroke	Volume	Flow Rate
Rear	40 mm	10 mm	20 mm	23.56 cm^3	2.83 l/min
Front	25 mm	10 mm	60 mm	24.74 cm^3	2.97 l/min

Table 1: Fluid volumes required to move the actuators.

To drive the pump, some advanced systems use an electric actuator powered by the motorcycle's battery. This approach allows for more precise and automated control, synchronized with the motorcycle's electronic control unit (ECU). It is also essential to select a compact and lightweight hydraulic pump. An appropriate solution could be the Parker F11-5, a fixed displacement hydraulic pump/motor with an inclined shaft, available in a displacement of 5 cm^3/rev. If the two actuators are in parallel, the total flow rate required by the pump is 5.80 l/min. This value represents the sum of the flow rates needed to simultaneously power both actuators. Therefore, a 5 cm^3/rev pump must rotate at approximately 1160 RPM to meet the system's requirements.

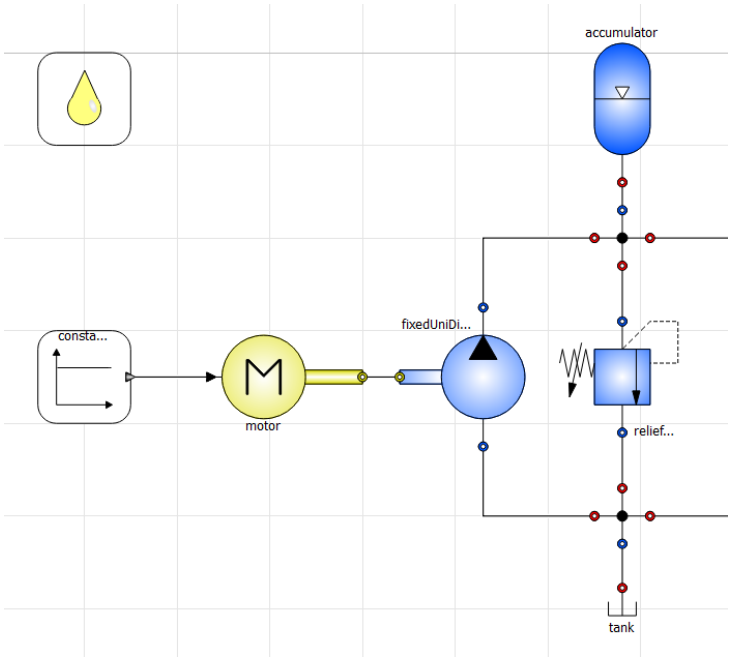


Figure 6: Generation group layout on OpenModelica.

Once the distribution group is loaded and the acceleration phase is complete, the motorcycle will face the most demanding operating condition for the system: braking. In this phase, almost the entire weight of the motorcycle and rider is transferred to the front, compressing the suspension, while the hydraulic circuit works to extend the fork. We will observe the first signs of extension in the moments following braking, which will then be overwhelmed by the load transfer to the front, causing the fork to compress again until the pump reaches the necessary power to return the motorcycle to its nominal setup.

To determine the required working pressure for the actuators, the values were calculated based on the dynamic loads transferred to the suspensions. For the rear lowering device, with a 40 mm piston, a 10 mm shaft, and a reduced load of 299.8 N (0.1 times the static load), the calculated pressure is 2.54 bar. For the front lowering device, with a 25 mm piston, a 10 mm shaft, and an increased load of 1972 N (1.9 times the static load), the pressure is 47.83 bar.

These calculations highlight how dynamic loads during braking significantly affect the pressures required by the hydraulic system. Compared to the previous case, a substantial increase in the electric motor's rotational speed is observed, necessary to provide the greater hydraulic power required. The motor will operate at a nominal speed of 1160 RPM, accelerating to 2320 RPM at the moment of braking, when the pump must deliver higher power. The doubling of the rotational speed is justified by the increase in operating pressure, which is approximately doubled under these conditions.

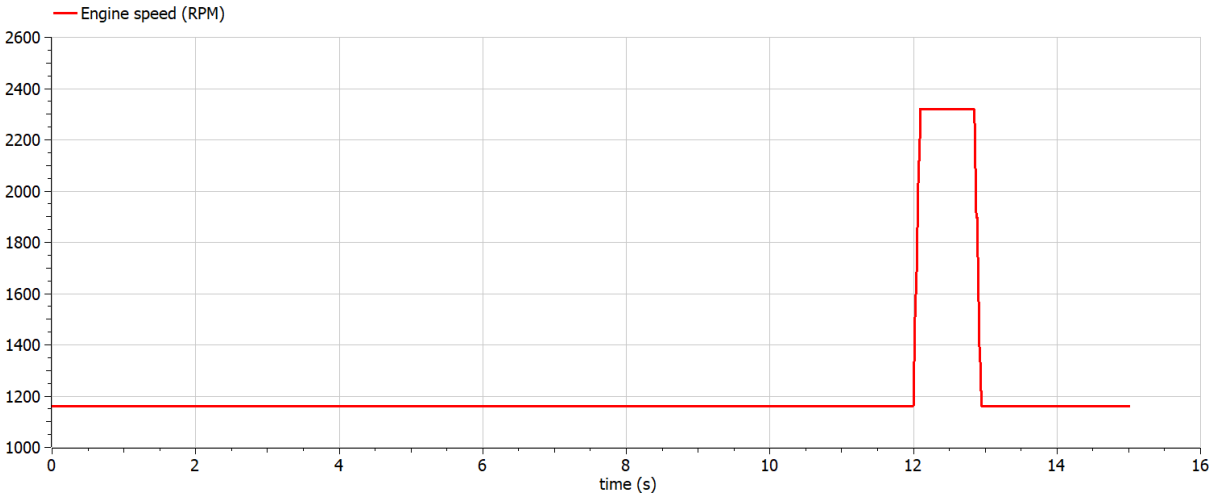


Figure 7: Engine speed variation during braking.

Since the maximum pressure recorded in the simulation is around 73.4 bar during braking, we will set the pressure relief valve at 100 bar as a precautionary measure to account for potentially more critical operating conditions, such as greater load transfer to the front, or issues like an increase in fluid temperature (which can increase viscosity), malfunctioning of the regulation valves, or a possible partial blockage of the pipes.

3.3 Fluid volume estimation

The choice of the internal diameter of the pipes in the lowering system was made by considering the maximum flow rate expected in the circuit and the operating pressure. The two parallel branches have flow rates of 2.83 l/min and 2.97 l/min, respectively, which are equivalent to:

$$Q_1 = \frac{2.83\,\text{l/min}}{60\,\text{s}} = 0.0472\,\text{l/s} = 4.72 \cdot 10^{-5}\,\text{m}^3/\text{s}$$
$$Q_2 = \frac{2.97\,\text{l/min}}{60\,\text{s}} = 0.0495\,\text{l/s} = 4.95 \cdot 10^{-5}\,\text{m}^3/\text{s}$$

Using a mean fluid velocity of 3 m/s, calculated as the optimal value to reduce pressure losses and ensure efficiency, the internal diameter of the pipes was determined using the formula:

$$d = \sqrt{\frac{4 \cdot Q}{\pi \cdot v}}$$

For the first pipe:

$$d_1 = \sqrt{\frac{4 \cdot 4.72 \cdot 10^{-5}}{\pi \cdot 3}} = 4.48\,\text{mm}$$

For the second pipe:

$$d_2 = \sqrt{\frac{4 \cdot 4.95 \cdot 10^{-5}}{\pi \cdot 3}} = 4.58\,\text{mm}$$

Based on these calculations, a standard internal diameter of 5 mm was chosen for both pipes. This value ensures adequate management of the maximum flow rate without excessively increasing pressure losses, with fluid velocity within the optimal range of 2-6 m/s. Assuming an operating pressure of 74 bar with peaks up to 100 bar, flexible hoses with an internal diameter of 5 mm (3/16") were selected, complying with the SAE 100 R5 standard. These hoses are designed for medium-pressure applications and offer the following characteristics:

- Maximum operating pressure: 207 bar, providing a large safety margin compared to the system's maximum pressure.
- Minimum burst pressure: 828 bar, higher than the system's operational requirements.
- Minimum bend radius: 76 mm, allowing flexibility and ease of installation.
- Operating temperature: from -40°C to +100°C, ensuring reliability under various operating conditions.

The SAE 100 R5 hoses consist of a synthetic rubber inner layer resistant to oils, a high-strength steel braid reinforcement, and an outer cover made of rubber-impregnated fabric, resistant to weathering. This configuration ensures high mechanical strength and long-term durability.

Assuming a length of 1 meter for both the supply and return lines for both the front and rear, the total fluid volume contained in them is calculated as follows:

$$V = \pi \cdot \left(\frac{d}{2}\right)^2 \cdot L_{\text{tot}} = 0.0785\,\text{l}$$

The total fluid volume contained in the circuit is approximately the sum of the volume in the pipes and the volume of the actuators. The volume in the pipes is 0.0785 l (approximately 78.5 ml). The volume of the actuators, previously determined, is 48.30 cm^3 (approximately 0.0483 l). By adding these contributions, the total volume of the circuit is:

$$V_{\text{totale}} = V_{\text{tubi}} + V_{\text{attuatori}} = 0.0785\,\text{l} + 0.0483\,\text{l} = 0.1268\,\text{l}$$

Therefore, the total volume of the circuit, required for the sizing of the pressure accumulator, is 0.1268 l (approximately 126.8 ml). A 200 ml pressure accumulator will be conservatively sized.

3.4 Distribution group

The engagement and disengagement signals of the lowering device are modeled through two linear stages, which transition from 0 to 1 in 0.1 seconds and vice versa. Engagement occurs via a button before departure, while disengagement happens during braking when the brake lever is activated. The system uses two 4/2 directional control valves:

- The activation valve is a normally closed valve with an open center, designed to ensure fluid recirculation under steady-state conditions while maintaining pressure in the downstream part of the circuit.
- The deactivation valve is a normally closed valve with a closed center, which allows the system to remain pressurized and to discharge only when necessary.

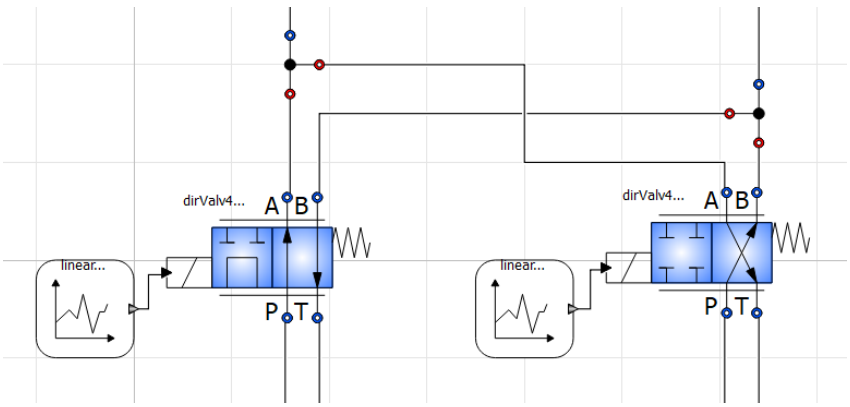


Figure 8: Distribution group layout on OpenModelica.

The activation signals of the distributors have been designed with rapidly increasing linear stages. The red color represents the time required to engage the lowering device with the motorcycle stationary, while the blue color identifies the time needed to return the motorcycle to normal conditions. The latter process takes more time as a single actuator must withstand a high load, and the pressures involved are higher.

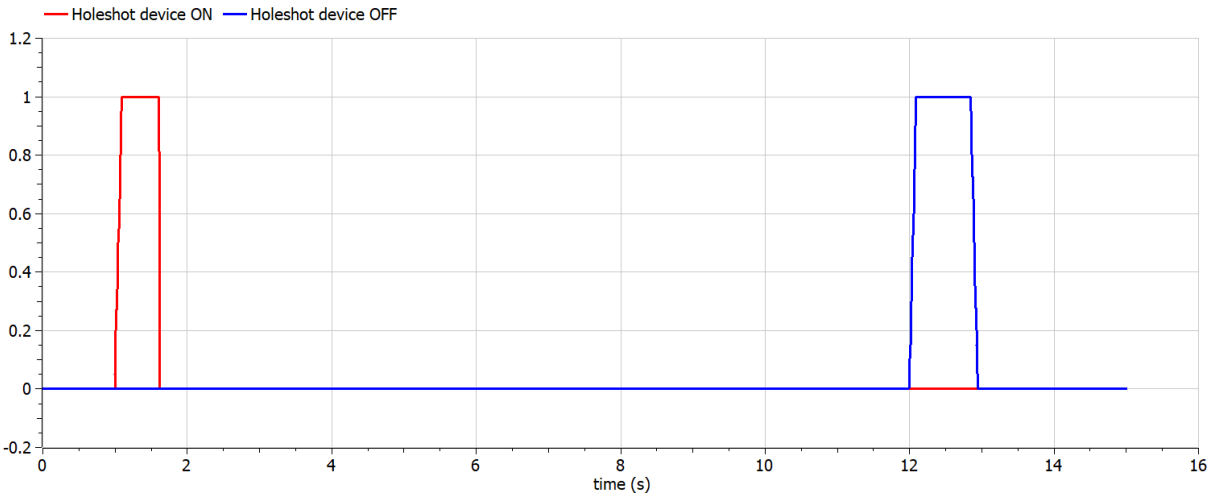


Figure 9: Holeshot device engagement/disengagement signals.

3.5 Execution group

For the rear, the modeling is simpler, as the actuator replacing the linkage is not significantly influenced by the dynamic effects of the shock absorber during the engagement phases considered in the simulation. However, a larger piston was chosen compared to the front one to handle the higher load resulting from the kinematics. The piston has a diameter of 40 mm, while the shaft has a diameter of 10 mm. The total stroke of the actuator is 50 mm, but it will move a negligible mass of 1 kg for an actual stroke of 20 mm.

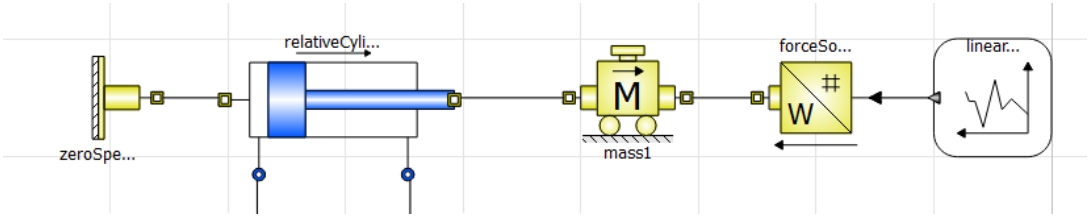


Figure 10: Rear execution group layout on OpenModelica.

For the front, an actuator was chosen with dimensions compatible with the oil chamber integrated into the suspension shaft. The actuator housing is fixed to the frame, which in this case corresponds to the shaft. The actuator's piston has a maximum stroke of 100 mm but is designed to impart an actual stroke of 60 mm to a negligible mass of 1 kg in

order to lower the motorcycle. The dynamic effects due to the elastic resistance of the spring and damping have been modeled through a combination of a spring and damper in parallel, subjected to the load transferred to the front end.

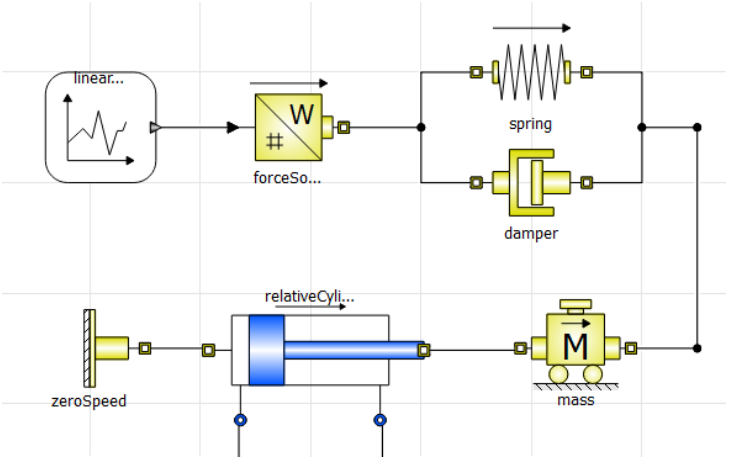


Figure 11: Front execution group layout on OpenModelica.

4 Main results

4.1 Pressure and stroke behavior

The behavior of the discharge pressure remains almost constant until braking, as the motorcycle naturally tends to lower when the suspensions are disabled, thus reducing the work of the pump. The pressure peak occurs at the braking point, when, as mentioned earlier, the electric motor's speed increases to transfer more power.

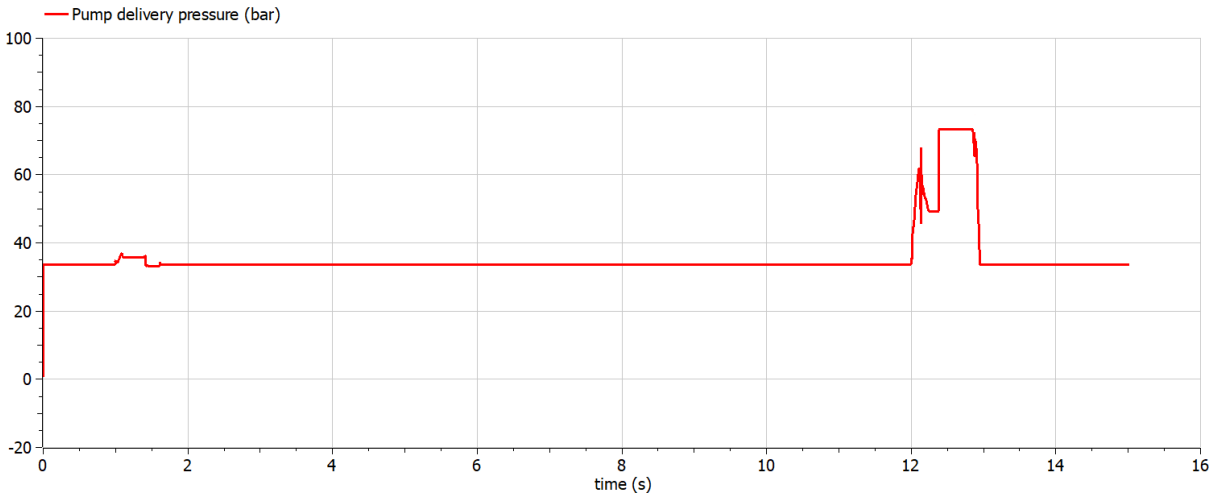


Figure 12: Discharge pressure behavior during the complete maneuver.

The stroke of the rear actuator, shown in blue, discharges rapidly during braking due to the pressure loss. The stroke of the front actuator, indicated in red, shows a slight extension at the beginning of braking, but the load transfer prevails thereafter. Once the pump increases power, the front fork begins to extend again.

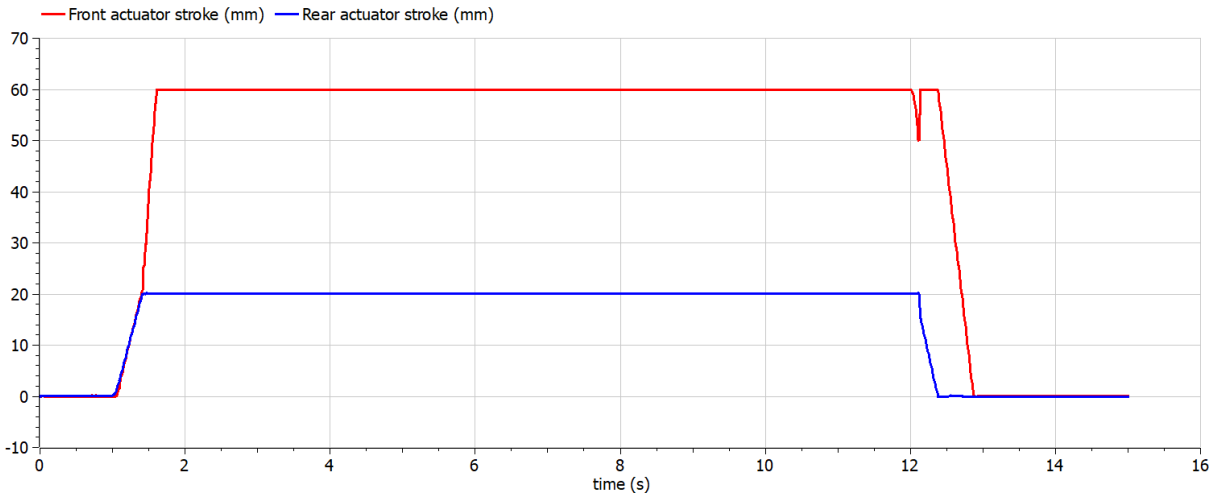


Figure 13: Actuators stroke behavior during the complete maneuver.

4.2 Complete circuit layout

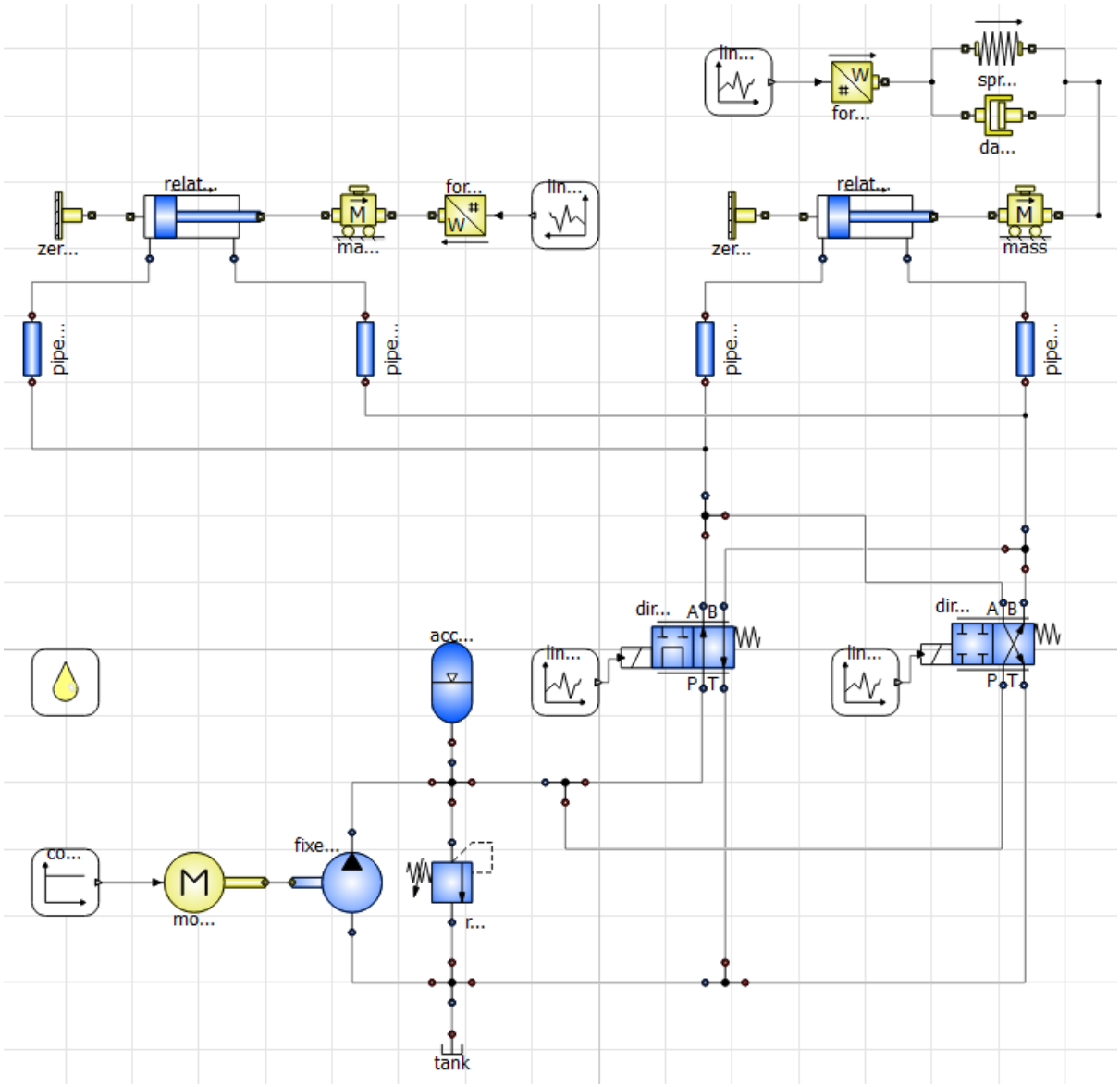


Figure 14: Holeshot device complete circuit layout.

References

- www.smartfluidpower.it - SmartFluidPower is a spin-off of the University of Modena and Reggio Emilia that provided a library of components for OpenModelica
- www.moto.it - MotoGP 2022. Bernardelle: "L'abbassatore Ducati, ecco cosa penso"
- www.rossomotori.it - L'abbassatore anteriore in MotoGP sarà abolito dal 2023
- www.wrs.it - Olio forcella Öhlins R&T 1309
- www.hydrover.it - Pompa idraulica serie F11-F12 a cilindrata fissa